Thermodynamic prediction of the effect of repeated recirculation of cooled flue gases on the content of major, minor, and trace compounds in oxy-coal combustion products

Wojciech Jerzak *

Abstract

This study investigates changes in the composition of oxy-coal combustion products resulting from the recirculation of cooled flue gas (FGR) at 20, 60, 100, 200, and 300 ^oC (containing 70–95 mol% CO_2). It presents the results of thermodynamic calculations describing changes in the content of the major, minor, and trace components of flue gases, ash and condensate. The results reflect a scenario of starting the oxy-coal combustion system in a fluidized bed boiler using low-purity oxygen from an air separation unit. This work demonstrates that in FGR loop the major species, i.e., Ar and N_2, as well as the minor, e.g., Cl_2, $PbCl_4$, $HgCl_2$, and $CrOCl_3$, are accumulated. After nine FGR loops cooled to 300 ^oC, marked increases in concentrations were observed: $ZnCl_2$ and HCl (3-fold), as well as $CrO_2(OH)_2$ (2.5-fold). The ash that was formed contained, among others, $CaSO_4$, SiO_2, $CaMgSi_2O_6$, $MgSiO_3$, $ZnFe_2O_4$, and $MgCr_2O_4$, whose mass changed in successive reactors as a result of the repeated FGR. Depending on the temperature of the cooling reactor, flue gases were subjected to recirculation and the main component of the condensate was H_2O or $H_2SO_4 \cdot 6H_2O$. The condensate contained chloride salts, e.g., $PbCl_2$, KCl, and $ZnCl_2$, as well as sulfate salts, i.e., K_2SO_4 and Na_2SO_4, in smaller amounts. A consequence of the nine-fold FGR cooled to $T \leq 200$ ^oC was, among others, a percentage mass increase in $ZnCl_2$ in the condensate. The less cooling applied to flue gases, the more likely the occurrence of sulfates was in the condensate.

Keywords: oxy-coal combustion, thermodynamic calculations, flue gas recirculation, fluidized bed boiler

1 Introduction

Carbon capture and storage (CCS) in coal-fired power plants is associated with costs related to capturing, transport, and storage. The profitability of CO_2 capture from flue gases increases when the amount of CO_2 in these gases is high. If one wants CO_2 to

*AGH University e-mail

predominate in the flue gases, the following technologies are used: chemical-looping combustion (CLC), pre-combustion capture, or oxy-fuel combustion, in which the oxidant is free of nitrogen. In terms of the pre-combustion capture or oxygen-fuel combustion technology, oxygen derived from air separation units (ASUs) acts as an oxidant [1]. In the oxy-coal combustion technology, in addition to oxygen, recirculated flue gases are transported to the boiler to decrease the flame temperature and increase the CO_2 concentration in the flue gases [2]. Because of recirculation, approximately 54.2 % − 80 % of the flue gases are recycled to the combustion chamber [3]; [4]; [5], and the remaining volume is redirected to the CO_2 purification unit. In the flue gases from oxy-fuel combustion, apart from CO_2 and H_2O, one can find decreased amounts of such chemicals as: O_2, SO_x, NO_x, N_2 (from the fuel and ASU), and Ar (from ASU) [6]; [7], along with trace amounts of HCl, Cl_2 [8]; [9], $HgCl_2$ [10], $AsCl_3$, CrO_2Cl_2, $PbCl_4$ [11], and $CrO_2(OH)_2$ [12]. The cooling of recirculated flue gases initiates the condensation of H_2O and H_2SO_4 [13], and of salts such as $PbCl_2$, $PbSO_4$, $ZnCl_2$ and $ZnSO_4$ [14] if the temperature drops below the dew point. The dew-point temperature from the oxy-coal combustion is higher than that of the flue gases emitted during coal combustion in air [5]. To reduce the condensation of moisture in the FGR loop, the temperature of the flue gases should be higher than 160 ^oC [3]; [4]. Because of the presence of water in flue gases, FGR may be dry or wet [15], or in different terminology, cold or warm [16]. FGR are usually divided into primary and secondary streams. The primary FGR stream should be sufficiently dry to be directed toward a coal transfer system without increasing its humidity after reaching a temperature not higher than 300 ^oC. Above 300 ^oC, the rolling-element bearings in carbon mills are damaged [3]. The secondary recycle stream is directed straight to the combustion chamber or can be mixed with oxygen. Considering the type of flue gases subjected to combustion and the type of boiler, FGR gases are cooled to 30 ^oC [10], 66 ^oC [17], 73 ^oC [18], and 100 ^oC [14], and can then be heated to 100 − 400 ^oC [3]; [15]. Recirculation of hot

flue gases provides more energy to the boiler, reducing costs of fuel supply and oxygen. In turn, the low temperature of purified flue gases ($25 - 75$ ^oC) is recommended in the adsorption of CO_2 on activated carbon. Inadequate purity of flue gases results in a decrease in CO_2 adsorption [19].

The FGR loop can accumulate SO_x, HCl, and H_2O, which adversely affects the operation of the installation [4]; [5]; [6]. One of the main substances contaminating flue gases is SO_2. If the concentration of SO_2 in the flue gases increases, there is a proportional increase in the SO_3 concentration in the boiler resulting in a decrease in the dew point of the flue gases [5].

The primary reason for carrying out the thermodynamic calculations for the products of oxy-fluidized coal combustion considering the application of the FGR loop is the lack of literature on the repeated recycling of non-purified cooled flue gases at different temperatures. Considering FGR at 20, 60, 100, 200, and 300 ^oC opens the way to evaluating the effect of the water vapor content in the flue gases on the composition of the combustion products (gaseous, solid, and liquid). Secondly, it facilitates the identification of components present in the combustion products in major, minor, and trace amounts, whose content varies in successive FGR loops. Thirdly, it demonstrates how the use of low-purity oxygen from the air separation unit (ASU) affects the composition of flue gases. The results presented in this paper give insight for both starting the fluidized bed boiler and evaluating air ingress into the boiler - which is unavoidable even at laboratory workstations [15]. The introduction provides an adequate literature review of the topic.

2 Materials and methods

2.1 Fuel

Polish hard coal was the fuel used in the study (medium - volatile bituminous coal - ASTM D388 per the Standard Classification of Coals by Rank). Table 1 presents a list of element masses per kilogram of dry coal calculated using the elemental and technical analysis of coal, as well as the ash analysis. The following major elements were identified in the coal under dry conditions: C, H, N, S, O, and Cl, along with lower amounts of Si, Fe, Al, Mn, Ti, Ca, Mg, P, Na, and P and trace amounts of As, Zn, Cr, Pb, Hg, and Cd. The hard coal studied met the fuel criteria required by the CFB Boiler Lagisza Power Plant 460 MWe with respect to the contents of moisture (6 % − 23 %), ash (10 % − 25 %), and sulfur (0.6 % − 1.4 %) [20].

Table 1: Elemental composition of 1-kg dry coal used in calculations

Elements	Mass
Major and Minor	(g/kg)
C	646.91
H	41.99
N	8.89
S	8.79
Cl	1.10
O*	190.73
Si	45.29
Al	29.45
Fe	10.19
K	7.07
Ca	4.03
Ti	1.96
Mg	1.60
Mn	1.25
Na	0.60
P	0.15
Trace	(mg/kg)
As	48
Zn	38
Cr	24
Pb	19.70
Hg	0.11
Cd	0.09

*Oxygen is calculated as a difference.

2.2 Calculation Concept

The objective of this study was to determine the effect of the repeated recirculation of cooled flue gases on the changes in the formation of oxy-coal combustion products. Thermodynamic calculations were based on a system of 20 reactors (10 combustion and 10 cooling reactors) connected in series in a sequence: combustion-cooling-combustion, according to Fig. 1.

Each of the combustion reactors with odd numbers from 1 to 19 reflects the process of oxy-combustion per kilogram of dry coal in a fluidized bed boiler at 850 ^oC and 0.1 MPa. Accordingly, the combustion process of 10 kg of dry coal took place in 10 reactors. The fuel composition for calculations based on thermodynamic equilibrium is always introduced as chemical elements [10]; [12]. The fuel moisture is deliberately omitted so as not to change the coal composition (according to Table 1) by increasing the mass of hydrogen and oxygen. For fuel oxidation, low-purity oxygen from ASU was delivered. Pure CO_2 was transferred to reactor 1 exclusively, while FGRs were transferred to the other reactors with odd numbers from 3–19. 52.5 g of $CaCO_3$ was injected into each combus-
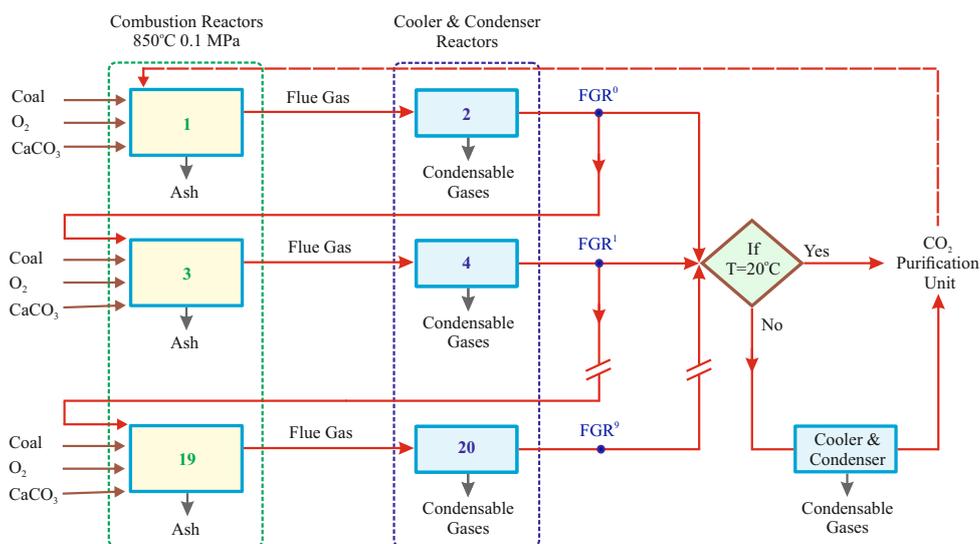
Figure 1: Simplified chart of the thermodynamic calculations

tion reactor to reduce the emission of SO_x. The mass of $CaCO_3$ added corresponded to the Ca/S molar ratio of 1.92, whose range was $1.9 \leq \frac{Ca}{S} \leq 3.0$, thereby facilitating the achievement of a capacity capture from Circulating Fluidized Bed Combustion (CFBC) of 90 % [20]. From each combustion reactor, the ash was distributed outside and the flue gases were condensed in the cooling reactor. The flue gas cooling reactors were assigned even numbers from 2 to 20. Five variants of flue gas cooling were adopted, particularly at 20, 60, 100, 200, and 300 ^oC. From each cooling reactor, the condensate was removed and the required FGR mass was directed to the following combustion reactor. The flue gases not recirculated entered the purification unit. To facilitate interpretation of the results of the flue gas composition calculations, after each recirculation loop, in Fig. 1, the following notation of points were introduced: FGR^0, FGR^1, ..., FGR^9. The notation of FGR^0 denotes the composition of cooled flue gases without recirculation after the combustion of 1 kg of coal, while FGR^1 represents the composition of cooled flue gases after the first recirculation loop and the combustion of 2 kg of coal.

2.3 Thermodynamic Tool, Databases, and Input Data

In this study, the thermodynamic equilibrium was modeled based on Gibbs' total free energy minimization. Thermodynamic prediction of the equilibrium phase formation during oxy-coal combustion was performed using the FactSage 6.3 software pack-

Table 2: Mass of substrates used in the calculations related to the combustion reactors

Reactor No.	1	3,5,...,19
Mass	(g)	(g)
Coal	1000.00	1000.00
CO_2	7331.15	0.00
FGR	0.00	7061.91
O_2	2070.01	1993.99
N_2	38.16	36.75
Ar	81.66	78.66
$CaCO_3$	52.50	52.50

age. FactSage 6.3 contains comprehensive ready-to-use thermochemical databases in different computational modules. This study used the "Equilib" module with databases such as FactPS, FTsalt, and FToxid. The following were entered into the Equilib module: (a) major, minor, and trace elements contained in the fuel according to Table 1, and (b) low-purity oxygen, CO_2 (only in the first reactor), FGR, and $CaCO_3$ according to Table 2.

The masses of O_2, N_2, and Ar were calculated from the composition of low-purity oxygen: 95 %v/v O_2, 2 %v/v N_2, and 3 %v/v Ar produced by Linde Engineering [21]. The ratio between low-purity oxygen and CO_2 (or FGR, starting from reactor 3) was assumed to be 23 wt.%/77 wt.%. To provide a comparison between the flue gas composition in the successive recirculation loops, a reference point describing the constant oxygen content in dry flue gases was established. In this study, the constant oxygen level in dry

flue gases established at 1.4 % v/vO_2 in each recirculation loop was achieved by ensuring a higher excess oxygen ratio ($\lambda = 1.1$) in the first combustion reactor than in the other reactors ($\lambda = 1.06$). The lower oxygen excess in combustion reactors 3–19 resulted from the fact that FGR gases contain oxygen.

3   Results and Discussion

The results of the thermodynamic calculations are presented sequentially for the flue gases, ash, and condensate. In the abovementioned oxy-combustion products, the compounds were classified by content, i.e., major, minor, and trace amounts.

3.1   Flue Gas

The results presented below refer to wet flue gases, which cooled to 20 ^oC, and contain 2.3 mol% water vapor (at each FGR point). The effect of the temperature of cooled wet flue gases on their density and volume is shown in Figs. 2(a) and (b).
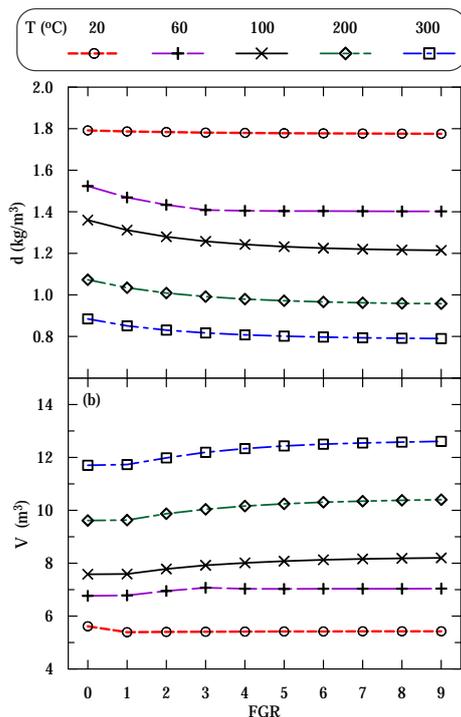
Figure 2: Density (a) and volume (b) of flue gases for successive FGR loops

The decrease in the density of flue gases is a consequence of FGR and leads to an increase in temperature. After nine recirculation loops of flue gases

($FGR^0 \rightarrow FGR^9$), the greatest decrease in density ($\Delta d = 0.15$) occurs at $T = 100\ ^oC$. In the first two recirculation loops (FGR^0–FGR^2), a significant decrease in density can be observed, which is evidently reported when $T \geq 60\ ^oC$. In contrast, a slight decrease in density was found for flue gases at $T = 20\ ^oC$. The higher the FGR temperature, the greater is their volume. In subsequent loops, the volume of FGR increases except for $T = 20\ ^oC$ within the range from FGR^0 to FGR^1. The main components of wet FGR gases are CO_2, H_2O, O_2, Ar, and N_2, and their proportion composition depends on the temperature, as shown in Figs. 3(a)–(e).

According to Fig. 3(a), the greatest amount of CO_2 (94.7 mol%) can be found in FGR cooled to 20 ^oC after combustion of the first kilogram of coal. In subsequent FGR loops, one can observe a loss of CO_2 resulting from the accumulation of Ar and N_2. Similar CO_2 content in FGR cooled to the temperatures of 100, 200, and 300 ^oC is observed in each loop of recirculation. Except for FGR at $T = 60\ ^oC$, as from the fourth recirculation loop (FGR^4) mol% CO_2 remains almost constant, which directly results from the unchanged content of H_2O, as demonstrated in Fig. 3(b). Water contained in the flue gases at 60 ^oC derived from FGR^4 begins to condense, which may indicate a decrease in the condensation point of flue gases. Flue gases cooled even to $T = 20\ ^oC$ contain 2.3 mol % H_2O at each FGR point. After combustion of 10-kg coal, in flue gases cooled to $T \geq 100\ ^oC$, one can find 70.2 % CO_2 and 24.2 % H_2O, which correlates with the literature values for wet flue gases: 68.5 % CO_2 and 27.7 % H_2O [22]. As reported in the literature, during oxy-coal combustion in wet FGR, up to 45 % H_2O was observed [23]. Although Fig. 3(c) shows changes in O_2 content in wet FGR, the oxygen content in dry flue gases remains constant (1.4 mol %) at each temperature and in each recirculation loop. The apparent influence of oxygen purity on the Ar and N_2 accumulation in consecutive FGR loops is shown in Figs. 3(d) and (e). The rate of oxygen and nitrogen accumulation depends on both oxygen purity and excess oxygen ratio (λ). The accumulation is facilitated via an increase in λ. The three components of FGR, namely, Cl_2, HCl, and $PbCl_4$, are compounds occurring in minor amounts. The volume of flue gases depends on the temperature and the changes in the subsequent FGR loops. Consequently, the concentration of compounds with lower content was expressed as a mass of the component with respect to the volume of flue gases as shown in Figs. 4 and 5(a)–(c).

The combustion of coal containing chlorine mainly results in the emission of atomic chlorine, which is converted into molecular chlorine [24]:
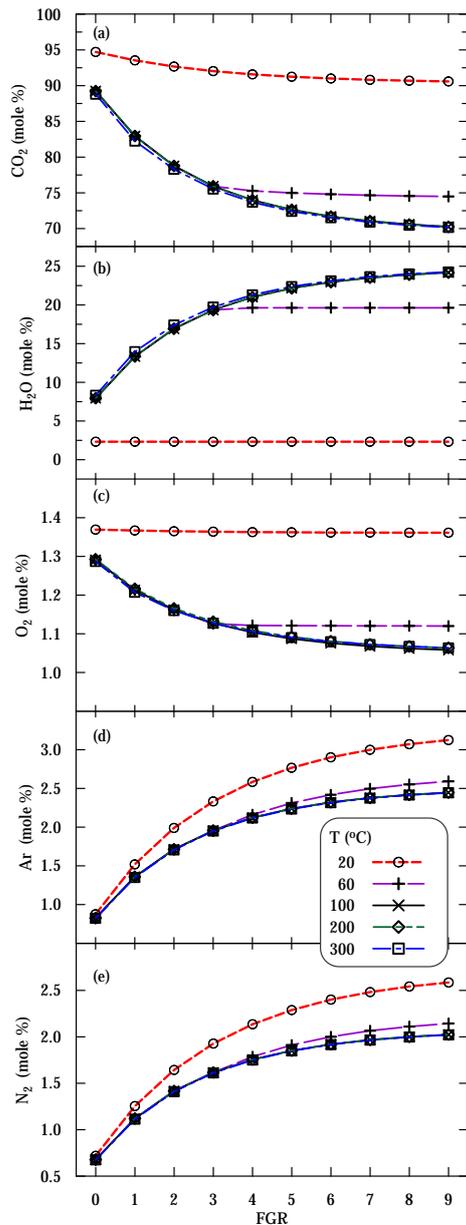
Figure 3: Mole percent of the main components of wet flue gases in subsequent FGR loops: (a) CO_2, (b) H_2O, (c) O_2, (d) Ar, and (e) N_2

$$2Cl \rightarrow Cl_2 \quad (1)$$
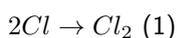
Alternatively, it forms HCl, among others, as a result of the following reaction [24]:

$$H + Cl \rightarrow HCl \quad (2)$$

$$4Cl + 2H_2O \rightarrow 4HCl + O_2 \quad (3)$$
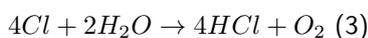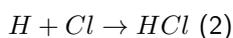
The calculation results confirm that decreasing the temperature of flue gases from 850 ^oC to 300 ^oC
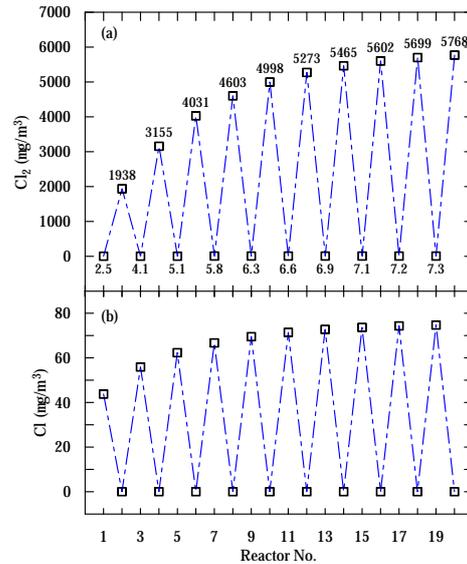
Figure 4: Changes in the content of (a) chlorine molecules and (b) atomic chlorine in successive FGR reactors at 300 ^oC

(as reflected in reactors 1–2, 3–4, etc.) results in an approximately 800-fold increase in the content of molecular chlorine with a simultaneous consumption of atomic chlorine, as demonstrated in Fig. 4. Cl_2 and HCl are the most important compounds responsible for the oxidation of Hg in flue gases [10]. As shown in Fig. 5, the concentrations of minor compounds strongly depend on the FGR temperature, since each of them achieves maximum concentration at a different temperature. If $T \leq 100$ ^oC, the concentration of molecular chlorine is higher than that of HCl, and vice versa, if $T \geq 200$ ^oC. Identical HCl concentrations in each cooling reactor were obtained for FGR at 200 and 300 ^oC. According to the literature, the concentration of HCl in flue gases ranges from 1 to 500 mg/m^3 [8]; [24] . In practice, most chlorides can be removed (up to 95 %) from flue gases in the wet flue gas desulfurization (FGD) system and approximately 3 % of these chlorides is condensed on fly ash particles [25]. In low-temperature flue gases, molecular chlorine becomes the most stable compound that can be produced as a result of the following Deacon reaction [24]; [26]:

$$4HCl + O_2 \rightarrow 2Cl_2 + 2H_2O \quad (4)$$
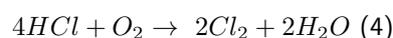
The interpretation of the calculation results depicts the chlorine consumption according to the following reaction [24]:

$$Cl_2 + SO_2 + H_2O \rightarrow 2HCl + SO_3 \quad (5)$$
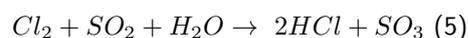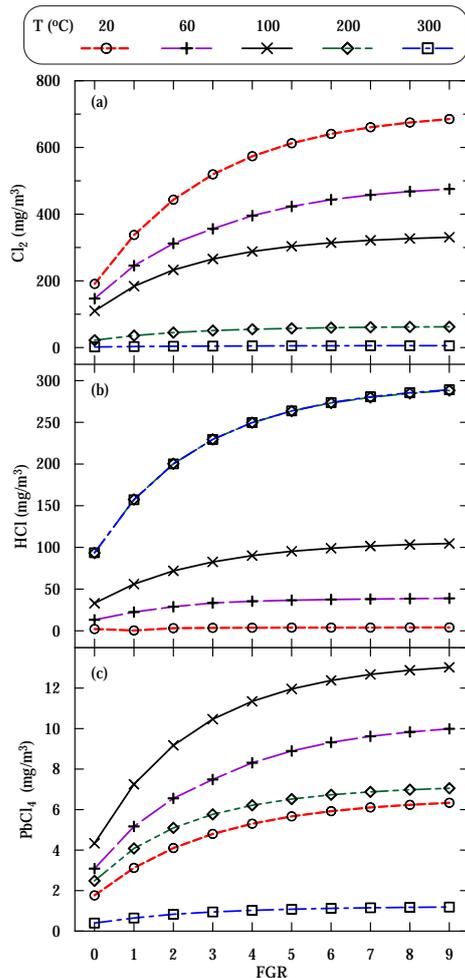
Figure 5: Concentrations of the following minor wet flue gas components in the subsequent FGR loops: (a) Cl_2, (b) HCl, and (c) $PbCl_4$

As a result of the flue gases cooling from 850 ^oC to 300 ^oC, the SO_2 concentration decreases at the expense of the formation of SO_3. Chlorine occurring in the combustion environment promotes the formation of metal chlorides [8]; [9]; [10] , as demonstrated by the calculation results: $PbCl_4$—Fig. 5(c); $ZnCl_2$ and CrO_2Cl_2—Figs. 6(a)–(c); and Zn_2Cl_4, $HgCl_2$, and $CrOCl_3$—Figs. 6(d)–(f). $PbCl_4$ is the dominant lead speciation in the FGR, which corresponds to the experimental results obtained for flue gases cooled below 300 ^oC [27]. As demonstrated by the thermodynamic calculations, the highest concentration of $PbCl_4$ is characterized by the FGR system cooled to 100 ^oC according to Fig. 5(c). After nine FGR loops, the concentration of $PbCl_4$ was 13 mg/m^3.

Among the trace compounds present in the FGR, six

are classified according to Figs. 6(a)–(f). A dominant trace compound in the FGR at 300 ^oC is $ZnCl_2$, whose concentration increases in the successive FGR loops and reaches the value of 2190 μg/m^3 (a three-fold increase in the concentration after nine recirculation loops). [10] and [14] confirmed the presence of $ZnCl_2$ in the cooling zones of flue gases at 365-155 ^oC and 600-300 ^oC . As demonstrated by the calculations, there is no $ZnCl_2$ in FGR cooled below 200°C, whereas a constant concentration (156 μg/m^3) in the successive FGR loops is observed only at $T = 200$ ^oC . At this temperature, an identical concentration is reported for Zn_2Cl_4, as shown in Fig. 6(d). Furthermore, the highest concentration of Zn_2Cl_4 can be found in FGR cooled to 200 ^oC.

Other compounds formed in the FGR in trace amounts are the speciation forms of hexavalent chromium (Cr^{6+}), i.e., CrO_2Cl_2 and $CrO_2(OH)_2$, as well as (Cr^{5+}), i.e., $CrOCl_3$, as shown in Figs. 6(b), (c), and (f). Further, Fig. 6(b) shows steady concentrations of CrO_2Cl_2 in two cases: after the first loop (FGR^1) for $T = 20$ ^oC, and after the fourth loop (FGR^4) for $T = 60$ ^oC. The concentration of CrO_2Cl_2 becomes constant precisely at the FGR points where water condensation begins, as discussed later in this paper. Further, CrO_2Cl_2 is a predominant trace compound in FGR at $T \leq 200$ ^oC. As observed in Fig. 6(c), the second position after $ZnCl_2$ in terms of the concentration in FGR at 300°C is occupied by $CrO_2(OH)_2$. After nine loops (FGR$^0 \rightarrow$ FGR^9), the concentration of $CrO_2(OH)_2$ increased by 2.5 times. The presence of water vapor in the oxygen-fuel atmosphere favors the formation of volatile $CrO_2(OH)_2$ according to the following reaction [28]:

$$2Cr_2O_3 + 3O_2 + 4H_2O \rightarrow 4CrO_2(OH)_2 \quad (6)$$
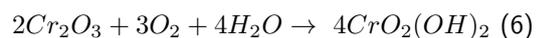
Mercury is present in flue gases mainly in the form of water-soluble $HgCl_2$ [26]. As shown in Fig. 6(e), the concentration of $HgCl_2$ exhibits a positive correlation with the cooling temperature of flue gases. The presence of Cl_2 and HCl in the FGR as well as the low temperature ($T < 400$ ^oC)[26] intensifies the oxidation of elemental mercury vapor (Hg^0) to $HgCl_2$ via the following reaction [26]; [12]:

$$Hg + Cl_2 \rightarrow HgCl_2 \quad (7)$$

$$2Hg + 4HCl + O_2 \rightarrow 2HgCl_2 + 2H_2O \quad (8)$$
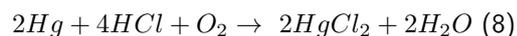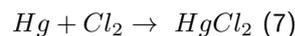
The last compound shown in Fig. 6(f) is $CrOCl_3$, whose concentration after nine recirculation loops did not exceed 50 μg/m^3. The highest concentration of $CrOCl_3$ was characterized by the FGR cooled to 100 ^oC. Moreover, note that in addition to the abovementioned compounds, only for FGR at $T = 300$ ^oC was the formation of $PbCl_2$ at the concentration of 386 μg/m^3 (FGR$^0 \rightarrow$ FGR^9) observed.
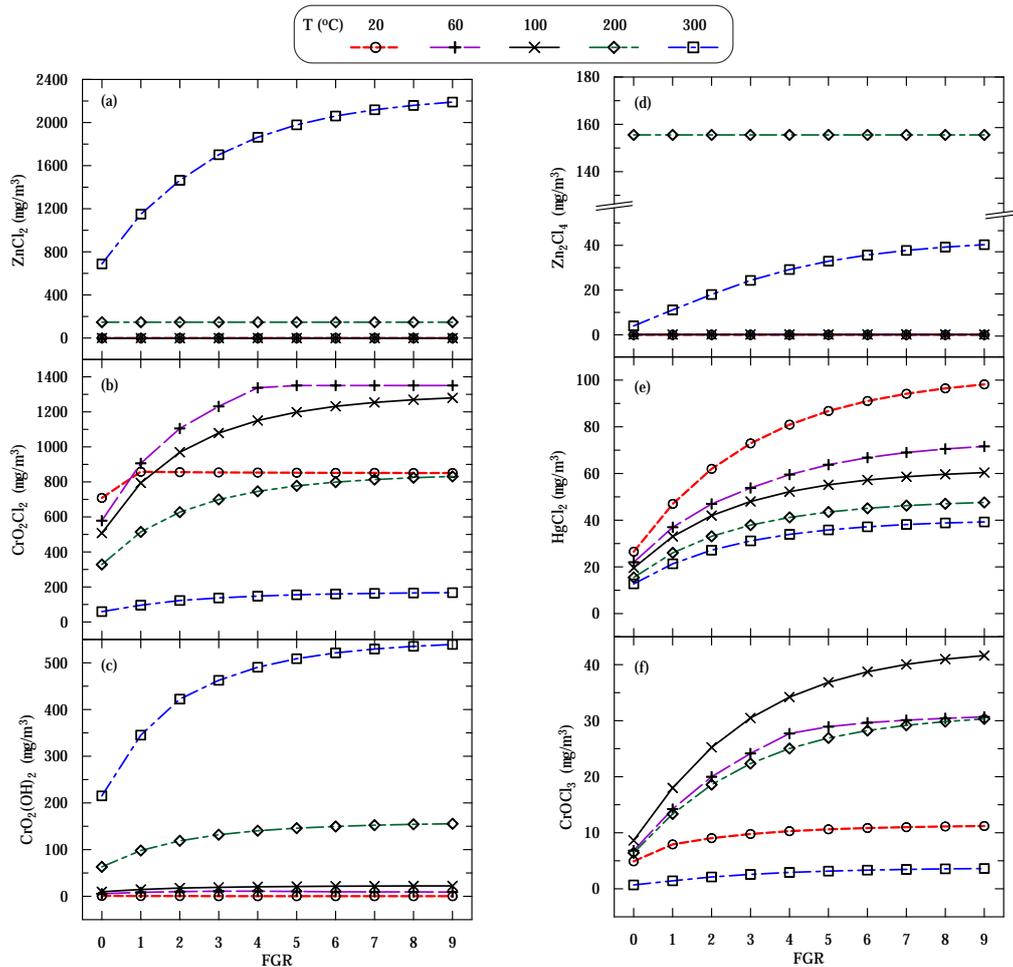
Figure 6: Concentration of trace compounds in wet flue gases in the subsequent FGR loops: (a) $ZnCl_2$, (b) CrO_2Cl_2, (c) Zn_2Cl_4, (d) $CrO_2(OH)_2$, (e) $HgCl_2$, and (f) $CrOCl_3$

3.2 Ash

As part of the calculations, one included the removal of the resulting ash from each combustion reactor according to the assumptions. This approach was used to evaluate the effect of the FGR temperature on the mass of ash forming in the subsequent reactors of coal combustion, as shown in Fig. 7. Identical ash mass (228.14 g) in reactor no. 1 for the considered FGR temperatures results from the same initial conditions as those assumed for the calculations. The mass of the ash formed in the subsequent combustion reactors does not change when the FGR temperature is 20 ^oC. If $60\ ^oC \leq T \leq 200\ ^oC$, a decrease in the mass of ash is observed in consecutive FGR loops. While for FGR at 300 ^oC, in reactors 3 and 5, one can observe an increase in the ash mass as a result of the formation of new compounds: $TiFe_2O_5$ (ferric pseudobrookite) and $Mg_2Al_4Si_5O_{18}$ (cordierite) instead of $CaSiTiO_5$

and $CaMgSi_2O_6$.
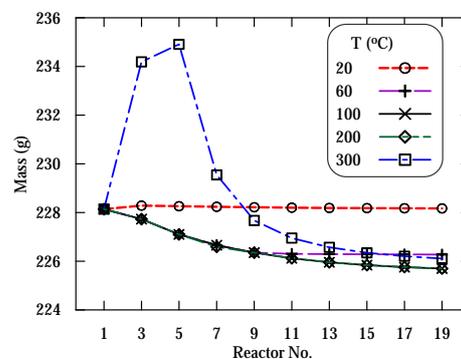
Figure 7: Mass of ash formed in the subsequent combustion reactors

Table 3: Masses of ash components formed in reactor 1

Species - crystalline phase	Mass
Major and minor	(g)
$CaAl_2Si_2O_8$ - anorthite	120.86
$KAlSi_2O_6$ - leucite	39.45
$CaSO_4$ - anhydrite	14.66
Fe_2O_3 - hematite	14.49
SiO_2 - quartz	8.41
$CaSiTiO_5$ - sphene	8.03
$CaMgSi_2O_6$ - diopside	7.53
$NaAlSi_3O_8$- high-albite	6.84
$Mn_3Al_2Si_3O_{12}$ - Mn-pyrop	3.75
$MgSiO_3$ - ortho-enstatite	3.1
Trace	(mg)
$Ca_3(PO_4)_2$ - whitlockite	751.1
$ZnFe_2O_4$	125.8
$AlAsO_4$	106.3
$MgCr_2O_4$- chromite	41.9

Ash formed in reactor 1 consists of 14 components (ten in major and minor amounts, and four in trace amounts), according to Table 3.

The predominance predominance of silicates results from an analysis of ash, whose main component is silicon, as previously reported in Table 1. Recent studies on coal-fired deposits under cooling conditions of flue gases confirm that the dominant compounds in ashes are silicates, i.e., $Ca_2Al_2SiO_7$, $CaMgSi_2O_6$, and sulfate $CaSO_4$ [29]. The ash components listed in Table 3 can be classified into two groups. The first group consists of compounds of unchangeable mass in all combustion reactors in the investigated FGR temperature range: $CaAl_2Si_2O_8$, $KAlSi_2O_6$, Fe_2O_3, $CaSiTiO_5$, $NaAlSi_3O_8$, $Mn_3Al_2Si_3O_{12}$, and $AlAsO_4$. Constant mass is also attributed to $Ca_3(PO_4)_2$ and $Ca_5(PO_4)_3(OH)$ (hydroxyapatite), but these compounds are not formed in all combustion reactors. Irrespective of the FGR temperature, the constituent ash component in all combustion reactors is $CaAl_2Si_2O_8$. The second group consists of ash components exhibiting a mass change at different FGR temperatures, as shown in Figs. 8(a)–(f).

When FGR temperature reaches 20 ^oC, the mass of compounds formed in ash:

- is almost constant in all the combustion reactors, e.g., $CaSO_4$, SiO_2, $CaMgSi_2O_6$, and $MgSiO_3$, according to Figs. 8(a)–(d), or in combustion reactors 5–19, i.e., $MgCr_2O_4$, according to Fig. 8(f), or,
- decreases in the subsequent combustion reactors, as for $ZnFe_2O_4$ (this compound is no longer formed in the last combustion reactor). Fur-

ther, $MgCr_2O_4$ is the only speciation form of chromium in ash, which is reflected in the calculations presented by [12].

When the FGR temperature is 60 ^oC, starting with combustion reactor 9 for $CaSO_4$, SiO_2, $CaMgSi_2O_6$, and $MgSiO_3$, and starting with reactor 11 for $MgCr_2O_4$, constant mass values were observed for the abovementioned compounds in ash. The mass of the ash components (except for $ZnFe_2O_4$) in the subsequent FGR loops remains constant if water is condensed from the flue gases, which is the case for FGR at 20 ^oC and 60 ^oC, as shown in Fig. 9(a). The highest sharp increase in the mass of $CaSO_4$, SiO_2, and $MgSiO_3$ occurs after the first FGR loop at 300 ^oC. A marked increase in $CaSO_4$ corresponds to the absence of $H_2SO_4 \cdot H_2O$ in the condensate, as shown in Fig. 9(b)

$CaSO_4$ is formed due to the addition of $CaCO_3$ to the combustion process. In oxy-fuel combustion conditions, direct sulfation of $CaCO_3$ is preferred [30]:

$$2CaCO_3 + 2SO_2 + O_2 \rightarrow \ 2CaSO_2 + 2CO_2 \quad (9)$$
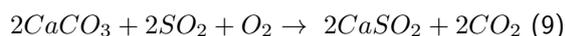
After the initial (in combustion reactor 3 with FGR at 300 ^oC) mass increase of SiO_2 and $MgSiO_3$, they decrease in the subsequent combustion reactors, mostly due to the formation of $CaMgSi_2O_6$ initiating in combustion reactor 7, according to Fig. 8(c).

3.3 Condensed gases

Sulfur and chlorine are acidic elements of coal. As a result of coal combustion, S and Cl (i.e., as SO_x and HCl) are transferred to the gradually cooled flue gases, thereby promoting the condensation of a condensate from the acid gas vapors. From the coolest flue gases, water condenses in each cooling reactor according to Fig. 9(a). However, for FGR at $T = 60\ ^oC$, water condensation initiates only in reactor 10, which might indicate a change in the dew point temperature. If the flue gases leaving the reactor exhibit a temperature higher than 60 ^oC, water does not condensate from the flue gases. A comparison of the results shown in Figs. 9(a) and (b) reveals that $H_2SO_4 \cdot 6\ H_2O$ is a major constituent of the condensate that forms when the flue gases cool to 60 ^oC (only for cooling reactors 4, 6, and 8), and higher than 60 ^oC for all cooling reactors. Furthermore, in each cooling reactor (irrespective of the FGR temperature), the salts whose total mass values are reported in Fig. 9(c) are condensed. The figure demonstrates that in the subsequent cooling reactors (when $T < 300\ ^oC$), the condensate contains a greater amount of salts. In reactor 20, the mass of the salts present in the condensate is almost four-fold higher than in reactor 2 for FGR at 20 ^oC.
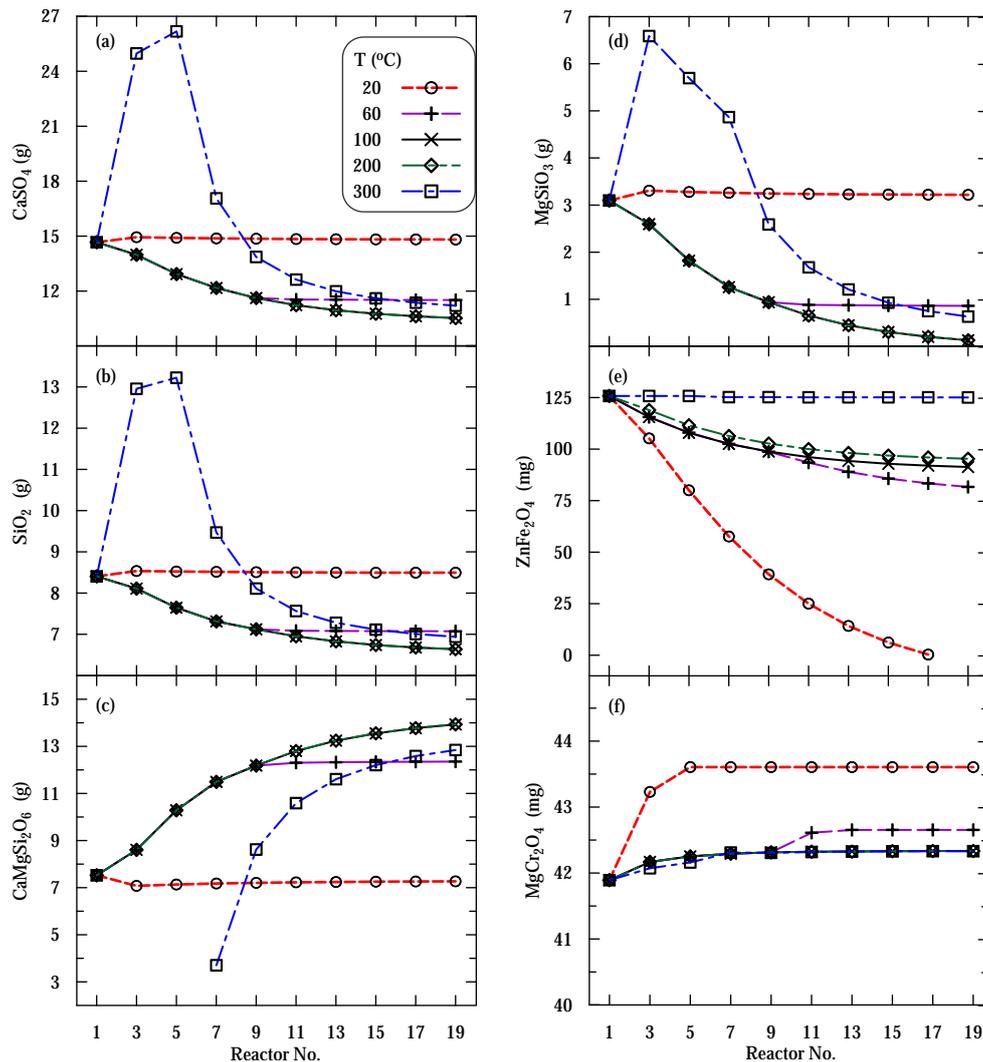
Figure 8: Minor and trace amounts of ash components formed in the subsequent combustion reactors: (a) CaSO$_4$, (b) SiO$_2$, (c) CaMgSi$_2$O$_6$, (d) MgSiO$_3$, (e) ZnFe$_2$O$_4$, (f) MgCr$_2$O$_4$

The effect of FGR temperature on the mass percentage of the salts present in the condensate in the subsequent cooling reactors is shown in Figs. 10(a)–(e). Further, ZnCl$_2$ is a predominant compound of the condensate when FGR is characterized by $T \leq 200\ ^oC$, while PbCl$_2$ is predominant for FGR at $300\ ^oC$. The more frequently the flue gases are subjected to recirculation, the higher the mass percentage of ZnCl$_2$ is in the condensate. The condensation temperature of ZnCl$_2$ is approximately $397\ ^oC$, while for PbCl$_2$, it is estimated to be around $527\ ^oC$ [22]. If the FGR $T \leq 100\ ^oC$, the condensate consists only of chlorides: PbCl$_2$, KCl, ZnCl$_2$, CdCl$_2$, MnCl$_2$, and NaCl. The higher FGR temperature (200 and $300\ ^oC$) promotes sulphates condensation: Na$_2$SO$_4$ and K$_2$SO$_4$.

At $300\ ^oC$, KCl and NaCl are not condensed from the flue gases, which indicates the conversion of chlorides into sulfates [20]; [22].

$$4KCl + 2SO_2 + O_2 + 2H_2O \rightarrow 2K_2SO_4 + 4HCl \quad (10)$$

$$4NaCl + 2SO_2 + O_2 + 2H_2O \rightarrow 2Na_2SO_4 + 4HCl \quad (11)$$
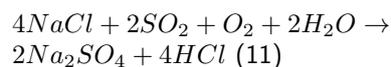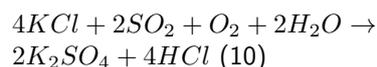
The course of the abovementioned reactions contributes to, among others, an increase in the HCl concentration in flue gases with the highest temperature, as shown in Fig. 5(b). In summary, the results of the calculations shown in Fig. 10 demonstrate that sulfate condensation is favored by the high temperature of
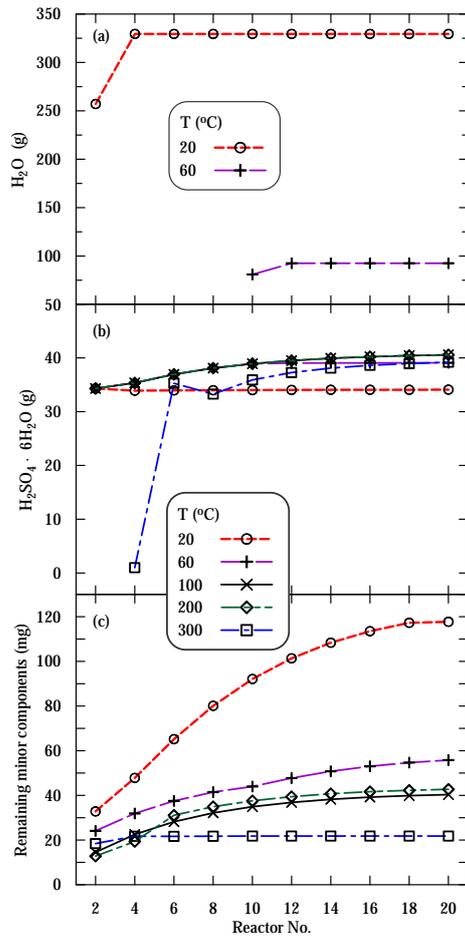
Figure 9: Masses of the major compounds condensed: (a) H_2O and (b) $H_2SO_4 \cdot 6H_2O$. (c) Sum of the masses of the other minor compounds in the subsequent cooling reactors

flue gases.

4 Conclusions

The major, minor, and trace compounds contained in the flue gases, ash, and condensate formed as a result of the oxy-coal combustion process using repeated FGR at different temperatures constituted the subject of this study. The thermodynamic calculations were performed using FactSage software. The presented results refer to a system of 20 reactors (10 combustion and 10 cooling reactors) connected in series in the following sequence: combustion-cooling-combustion. For each of the combustion reactors, 1 kg of coal was transported; the process of coal combustion was analyzed for 10 kg of coal.

The major conclusions from the calculations were as follows:

- In the flue gases, the following compounds were distinguished: (a) major - CO_2, H_2O, O_2, Ar, and N_2, (b) minor - Cl_2, HCl, and $PbCl_4$, and (c) trace compounds - $ZnCl_2$, CrO_2Cl_2, $ZnCl_4$, $CrO_2(OH)_2$, $HgCl_2$, and $CrOCl_3$. The maximum content of CO_2 in the flue gases estimated to be 94.7 mol% was obtained for the cooling system having a temperature of up to 20 ^oC in reactor 1 (i.e., without recirculation). As a result of the Ar and N_2 accumulation in the flue gases in the subsequent FGR loops, a reduction in CO_2 content was observed. The lower the flue gas temperature, the higher the molecular chlorine content was. After nine loops of FGR cooled to 300 ^oC, a three-fold increase was observed in the $ZnCl_2$ and HCl concentrations.
- Ash formed from the oxy-coal combustion process consisted of 14 components. In the last combustion reactor, the highest ash mass of 1 kg of coal was obtained when the FGR was cooled to 20 ^oC. Repeated FGR led to mass changes of the formed ash components: $CaSO_4$, SiO_2, $CaMgSi_2O_6$, $MgSiO_3$, $ZnFe_2O_4$, and $MgCr_2O_4$.
- The condensate composition largely depended on the FGR temperature and the changes in the subsequent cooling reactors. If the flue gases leaving the reactor were characterized by a temperature above 60 ^oC, water did not condense from the flue gases. In each cooling reactor (irrespective of the temperature and FGR loop), the condensation of salts was observed.

Acknowledgements
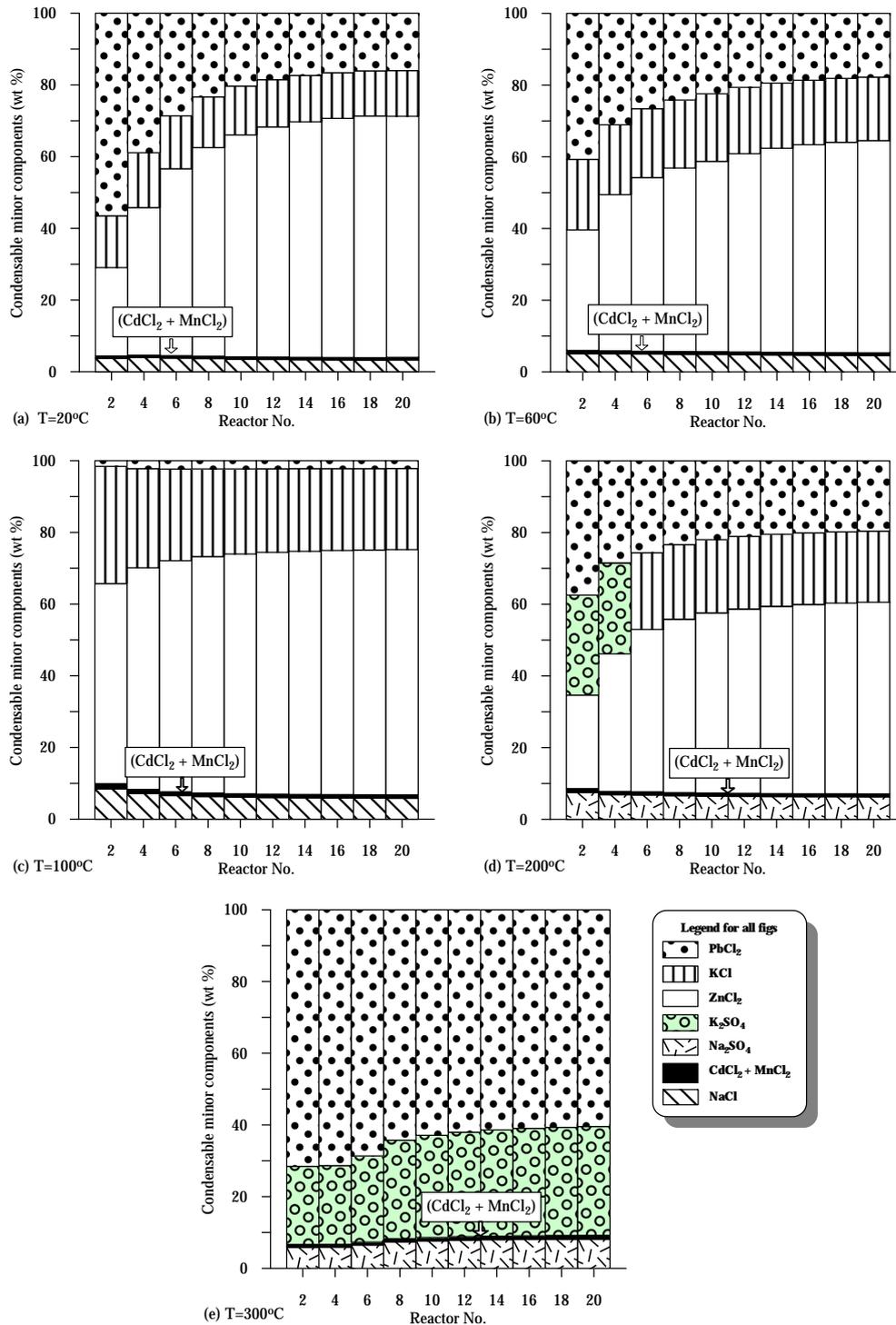
Figure 10: Condensable minor components in the subsequent cooling reactors with temperatures: (a) 20 ^{o}C, (b) 60 ^{o}C, (c) 100 ^{o}C, (d) 200 ^{o}C, and (e) 300 ^{o}C

References

1.Gładysz, P., and Ziebik, A. (2015) *Complex exergy analysis of an integrated oxy-fuel combustion power plant with CO2 transport and storage*.

2.Nemitallah, M.A., Habib, M.A., Badr, H.M., Said,

S.A., Jamal, A., Ben-Mansour, R., Mokheimer, E.M.A., and Khaled, M. (2017) Oxy-fuel combustion technology: current status applications, and trends. *International Journal of Energy Research*, **41** (12), 1670–1708.

3.Dillon, D.J., White, V., Allam, J.A., Rodney, Wall, R.A., and Gibbins, J. (2005) Oxy Combustion Processes for CO2 Capture from Power Plant, Technical Report 2005/9.

4.Duan, L., Sun, H., Zhao, C., Zhou, W., and Chen, X. (2014) Coal combustion characteristics on an oxy-fuel circulating fluidized bed combustor with warm flue gas recycle. *Fuel*.

5.Hu, Y., Yan, J., and Li, H. (2012) Effects of flue gas recycle on oxy-coal power generation systems. *Applied Energy*.

6.Wall, T., Liu, Y., Spero, C., Elliott, L., Khare, S., Rathnam, R., Zeenathal, F., Moghtaderi, B., Buhre, B., Sheng, C., Gupta, R., Yamada, T., Makino, K., and Yu, J. (2009) An overview on oxyfuel coal combustion-State of the art research and technology development. *Chemical Engineering Research and Design*, **87** (8), 1003–1016.

7.Font-Palma, C., Errey, O., Corden, C., Chalmers, H., Lucquiaud, M., Sanchez del Rio, M., Jackson, S., Medcalf, D., Livesey, B., Gibbins, J., and Pourkashanian, M. (2016) Integrated oxyfuel power plant with improved CO2 separation and compression technology for EOR application. *Process Safety and Environmental Protection*, **103** (Part B), 455–465.

8.Córdoba, P., Maroto-Valer, M., Delgado, M.A., Diego, R., Font, O., and Querol, X. (2016) Speciation, behaviour, and fate of mercury under oxy-fuel combustion conditions. *Environmental Research*, **145**, 154–161.

9.Sun, J.Q., Crocker, C.R., and Lillemoen, C.M. (2000) The effect of coal combustion flue gas components on low-level chlorine speciation using EPA Method 26A. *Journal of the Air and Waste Management Association*, **50** (6), 936–940.

10.Jano-Ito, M.A., Reed, G.P., and Millan, M. (2014) Comparison of thermodynamic equilibrium predictions on trace element speciation in oxy-fuel and conventional coal combustion power plants. *Energy and Fuels*, **28** (7), 4666–4683.

11.Suriyawong, A. (2009) Oxy-Coal Combustion : Submicrometer Particle Formation , Mercury Speciation , And Their Capture. *Thesis*, (August 2009).

12.Roy, B., Choo, W.L., and Bhattacharya, S. (2013) Prediction of distribution of trace elements under Oxy-fuel combustion condition using Victorian brown coals. *Fuel*, **114**, 135–142.

13.Xiang, B., Zhang, M., Yang, H., and Lu, J. (2016) Prediction of Acid Dew Point in Flue Gas of Boilers Burning Fossil Fuels. *Energy and Fuels*, **30** (4), 3365–3373.

14.Song, W., Jiao, F., Yamada, N., Ninomiya, Y., and Zhu, Z. (2013) Condensation behavior of heavy metals during oxy-fuel combustion: Deposition, species distribution, and their particle characteristics. *Energy and Fuels*, **27** (10), 5640–5652.

15.Toftegaard, M.B., Brix, J., Jensen, P.A., Glarborg, P., and Jensen, A.D. (2010) Oxy-fuel combustion of solid fuels. *Progress in Energy and Combustion Science*, **36** (5), 581–625.

16.Wang, H., Duan, Y., Li, Y. ning, Xue, Y., and Liu, M. (2016) Investigation of mercury emission and its speciation from an oxy-fuel circulating fluidized bed combustor with recycled warm flue gas. *Chemical Engineering Journal*, **300**, 230–235.

17.Seltzer, A., Fan, Z., and Archie, R. (2006) Conceptual Design of Supercritical O 2 -Based PC Boiler Final Report. (November), 1–165.

18.Hagi, H., Nemer, M., Le Moullec, Y., and Bouallou, C. (2013) Assessment of the flue gas recycle strategies on oxy-coal power plants using an exergy-based methodology. *Chemical Engineering Transactions*, **35**, 343–348.

19.Majchrzak, A., and Nowak, W. (2017) Separation characteristics as a selection criteria of CO2 adsorbents. *Journal of CO2 Utilization*, **17**, 69–79.

20.Hotta, A. (2009) *Foster Wheeler's Solutions for Large Scale CFB Boiler Technology: Features and Operational Performance of Łagisza 460 MWe CFB Boiler*, Springer.

21.Goloubev, D. (2012) Oxygen production for oxy-fuel power plants. Status of development. *2nd International Workshop on Oxyfuel FBC Technology, June 28-29th 2012, IFK University of Stuttgart*.

22.Meng, Y., Liang, X., Zhang, L., Jiao, F., Kumita, M., Namioka, T., Yamada, N., Sato, A., and Ninomiya, Y. (2015) Condensation behavior of heavy metal vapors upon flue gas cooling in oxy-fuel versus air combustion. *Journal of Chemical Engineering of Japan*, **48** (6), 450–457.

23.Jiang, Z., Duan, L., Chen, X., and Zhao, C. (2013) Effect of water vapor on indirect sulfation during oxy-fuel combustion. *Energy and Fuels*, **27** (3), 1506–1512.

24. Dranga, B.A., Lazar, L., and Koeser, H. (2012) Oxidation catalysts for elemental mercury in flue gases - A review. *Catalysts*, **2** (1), 139–170.

25. Cheng, C.M., Hack, P., Chu, P., Chang, Y.N., Lin, T.Y., Ko, C.S., Chiang, P.H., He, C.C., Lai, Y.M., and Pan, W.P. (2009) Partitioning of mercury, arsenic, selenium, boron, and chloride in a full-scale coal combustion process equipped with selective catalytic reduction, electrostatic precipitation, and flue gas desulfurization systems. *Energy and Fuels*, **23** (10), 4805–4815.

26. Wu, J., Cao, Y., Pan, W., and Pan, W. (2015) The Status of Mercury Emission from Coal Combustion Power Station. *In Coal Fired Flue Gas Mercury Emission Controls*, pp. 19–30.

27. Sakano, T., Furuuchi, M., Hata, M., Kanaoka, C., and Yang, K.-S. (2015) Separation Characteristics of Heavy Metal Compounds by Hot Gas Cleaning. *Proc. of 5th International Symposium on Gas Cleaning at High Temperature*.

28. Opila, E.J., Myers, D.L., Jacobson, N.S., Nielsen, I.M.B., Johnson, D.F., Olminsky, J.K., and Allendor, M.D. (2007) Theoretical and experimental investigation of the thermochemistry of CrO2(OH)2(g). *Journal of Physical Chemistry A*, **111** (10), 1971–1980.

29. Kinnunen, H., Hedman, M., Engblom, M., Lindberg, D., Uusitalo, M., Enestam, S., and Yrjas, P. (2017) The influence of flue gas temperature on lead chloride induced high temperature corrosion. *Fuel*, **196**, 241–251.

30. Fleig, D., Andersson, K., Johnsson, F., and Leckner, B. (2011) Conversion of sulfur during pulverized oxy-coal combustion. *Energy and Fuels*, **25** (2), 647–655.